# Mechanisms of the Tropical Upwelling Branch of the Brewer–Dobson Circulation: The Role of Extratropical Waves

GANG CHEN AND LANTAO SUN

*Department of Earth and Atmospheric Sciences, Cornell University, Ithaca, New York*

(Manuscript received 2 February 2011, in final form 20 May 2011)

ABSTRACT

The role of extratropical waves in the tropical upwelling branch of the Brewer–Dobson circulation is investigated in an idealized model of the stratosphere and troposphere. To simulate different stratospheric seasonal cycles of planetary waves in the two hemispheres, seasonally varying radiative heating is imposed only in the stratosphere, and surface topographic forcing is prescribed only in the Northern Hemisphere (NH). A zonally symmetric version of the same model is used to diagnose the effects of different wavenumbers and different regions of the total forcing on tropical stratospheric upwelling.

The simple configuration can simulate a reasonable seasonal cycle of the tropical upwelling in the lower stratosphere with a stronger amplitude in January (NH midwinter) than in July (NH midsummer), as in the observations. It is shown that the seasonal cycle of stratospheric planetary waves and tropical upwelling responds nonlinearly to the strength of the tropospheric forcing, with a midwinter maximum under strong NH-like tropospheric forcing and double peaks in the fall and spring under weak Southern Hemisphere (SH)-like forcing. The planetary wave component of the total forcing can approximately reproduce the seasonal cycle of tropical stratospheric upwelling in the zonally symmetric model.

The zonally symmetric model further demonstrates that the planetary wave forcing in the winter tropical and subtropical stratosphere contributes most to the seasonal cycle of tropical stratospheric upwelling, rather than the high-latitude wave forcing. This suggests that the planetary wave forcing, prescribed mostly in the extratropics in the model, has to propagate equatorward into the subtropical latitudes to induce sufficient tropical upwelling. Another interesting finding is that the planetary waves in the summer lower stratosphere can drive a shallow residual circulation rising in the subtropics and subsiding in the extratropics.

## 1. Introduction

Tropospheric air and chemical constituents enter the stratosphere primarily through the tropical upwelling branch of the Brewer–Dobson circulation (BDC) (Brewer 1949; Dobson 1956). The upward motion in the tropical stratosphere leads to adiabatic cooling, which controls a tropical cold point at the tropopause and consequently determines the mixing ratio of water vapor entering the stratosphere. In addition to climatological tropical upwelling, stronger upwelling can be inferred during January than during July near the tropical cold point (Reed and Vicek 1969), in the residual circulation derived from the thermodynamic balance (e.g., Rosenlof 1995; Randel et al. 2008), and in the mixing ratios of water vapor, ozone, and other chemical species in the tropical lower stratosphere (e.g., Mote et al. 1996; Niwano 2003; Randel et al. 2007; Schoeberl et al. 2008).

Recently developed chemistry–climate models, with improved representation of stratospheric chemistry and climate, almost unanimously predict an acceleration of the BDC and a decrease of the age of stratospheric air under climate change (e.g., Butchart et al. 2006; Li et al. 2008; Garcia and Randel 2008; McLandress and Shepherd 2009; Butchart et al. 2010). Although there is no evidence of trend in the age of stratospheric air derived from balloon-borne measurements of stratospheric trace gases (Engel et al. 2008), the mean age trends estimated from the observations have large uncertainties due to sparse spatial sampling (Garcia et al. 2010; Ray et al. 2010). An improved understanding of the dynamics of tropical stratospheric upwelling is critical for the prediction of future changes in stratospheric chemistry and climate. In this paper, we investigate the dynamics of BDC in an idealized model of the stratosphere and troposphere.

*Corresponding author address:* Gang Chen, Department of Earth and Atmospheric Sciences, Cornell University, Ithaca, NY 14853.
E-mail: gc352@cornell.edu

DOI: 10.1175/JAS-D-11-044.1

It is well recognized that the BDC is fundamentally governed by the angular momentum balance in the stratosphere. In the absence of wave drag, the BDC may be driven by nonlinear thermally driven circulations, analogous to tropospheric Hadley cell circulations, and this appears to be particularly important for the tropical upwelling in the summer hemisphere or in the upper stratosphere (Dunkerton 1989; Semeniuk and Shepherd 2001a,b; Tung and Kinnersley 2001; Zhou et al. 2006). More importantly, wave drag (i.e., planetary-scale, synoptic-scale, or gravity wave drag) can contribute to the forcing of the BDC through the downward control principle (Haynes et al. 1991; Holton et al. 1995; Plumb 2002).

Through the downward control mechanism, transient high-latitude wave forcing may induce a broad residual circulation extending into the tropics. Randel et al. (2002a,b) showed the observational evidence that week-to-week fluctuations in the high-latitude wave forcing can induce tropical upwelling. Furthermore, tropical upwelling has been found to be correlated with the high-latitude eddy forcing for the annual cycle (Yulaeva et al. 1994; Chae and Sherwood 2007) and interannual variability (Salby and Callaghan 2002; Dhomse et al. 2008). Based on additional statistical analysis, Ueyama and Wallace (2010) concluded that high-latitude planetary wave forcing plays an important role in modulating the tropical upwelling of the BDC on the subseasonal, seasonal, and interannual time scales. Along the same lines, Lin et al. (2009) and Fu et al. (2010) argued that the strengthening of the BDC, inferred from satellite-retrieved stratospheric temperature records, is caused by the trend in high-latitude eddy heat fluxes.

However, the downward control mechanism also says that the residual circulation should be confined in the latitude band of the forcing, provided that the wave drag is much more persistent than the radiative damping time scale. Therefore, it requires the extratropical wave drag to extend to the subtropical latitudes or some form of tropical wave drag to generate realistic tropical upwelling on the seasonal or longer time scales (Plumb and Eluszkiewicz 1999; Semeniuk and Shepherd 2001a; Scott 2002; Zhou et al. 2006; Geller et al. 2008). Along this line, Garcia and Randel (2008) argued that the increased subtropical wave drag, due to stronger subtropical lower stratospheric zonal winds under climate warming, can explain the trend of tropical upwelling. In an idealized aquaplanet atmospheric model, Chen et al. (2010) imposed different zonally symmetric sea surface temperature (SST) warming profiles and found that the increased subtropical zonal winds are indeed important for the increased strength in the BDC associated with synoptic waves.

Since both extratropical waves and tropical waves are important for the zonal momentum balance in the tropical upwelling (Randel et al. 2008; Taguchi 2009), seasonally varying equatorial deep convections and their associated planetary waves are also put forward to explain the annual cycle in tropical upwelling (Boehm and Lee 2003; Kerr-Munslow and Norton 2006; Norton 2006). Extending this line of argument, Deckert and Dameris (2008), Rosenlof and Reid (2008), and Garny et al. (2009) have suggested that the secular tropical SST warming and more vigorous tropical convection could lead to a strengthening of the BDC.

Given different perspectives on the mechanisms of tropical stratospheric upwelling, we utilize a mechanistic model of the stratosphere–troposphere system to investigate the role of extratropical waves in the dynamics of the tropical upwelling. A zonally symmetric version of the same model is used to diagnose the residual circulation associated with different branches of the total eddy forcing.

The paper is organized as follows. First, we briefly summarize the dynamical balance between tropical stratospheric upwelling and dynamical cooling in section 2. Next, the idealized atmospheric model and its characteristics are described in section 3. The simulations of tropical upwelling in the full model are presented in section 4, and the dynamics of upwelling is analyzed in section 5 using the zonally symmetric version of the full model. A brief summary and discussion are provided in section 6. The zonally symmetric model is described in the appendix.

## 2. Tropical stratospheric upwelling and dynamical cooling

We diagnose the residual circulations using the dynamical temperature changes in the primitive equations. The relation between the two can be illustrated using the zonal mean equations of the atmosphere in a transformed Eulerian mean (TEM) framework (e.g., Andrews et al. 1987) as

$$\begin{aligned} \frac{\partial \overline{u}}{\partial t} - \hat{f}\overline{v}^* &= \overline{G}, \\ \frac{1}{a\cos\phi}\frac{\partial(\overline{v}^*\cos\phi)}{\partial\phi} + \frac{1}{\rho_0}\frac{\partial(\rho_0\overline{w}^*)}{\partial z} &= 0, \\ \frac{\partial \overline{T}}{\partial t} + \overline{w}^*\left(\frac{HN^2}{R}\right) &= -\frac{\overline{T} - T_{\rm eq}}{\tau_E}, \end{aligned} \quad (1)$$

where $\hat{f} = f_0 + \overline{\zeta}$ is the absolute vorticity, $\overline{G}$ is the wave drag, $T_{\rm eq}$ is the radiative equilibrium temperature, $\tau_E$ is the radiative relaxation time scale, and other symbols adopt the meteorological convention. The absolute vorticity is related to the meridional gradient of the angular momentum $M$ by $\hat{f} = 1/(a^2\cos\phi)(\partial M/\partial\phi)$.

The downward control principle states that the residual vertical velocity can be diagnosed by combining the momentum and mass continuity equations (Haynes et al. 1991; Holton et al. 1995; Randel et al. 2002a):

$$\overline{w}^* = -\frac{1}{\rho_0 a \cos\phi}\frac{\partial}{\partial\phi}\left[\cos\phi\int_z^\infty \frac{\rho_0}{\hat{f}}\left(\overline{G} - \frac{\partial\overline{u}}{\partial t}\right)dz'\right]. \quad (2)$$

This suggests that the time mean residual circulation is confined by the latitude band of $\overline{G}$, and that the upwelling is more efficient as the drag extends into the deeper tropics (smaller $\hat{f}$).

The residual vertical velocity induced by the wave drag can also be inferred through a thermodynamic balance between the adiabatic motion and radiative heating (e.g., Rosenlof 1995). The eddy-induced temperature can be defined as $T_{\rm dyn} = T - T_{\rm rad}$. Here $T_{\rm rad}$ is the temperature in an eddy-free simulation, in which $\overline{G}$ and the associated eddy-driven residual circulation are set to zero. The difference between $T_{\rm rad}$ and $T_{\rm eq}$ is small in the extratropics, but it can be nonnegligible in the deep tropics because of the thermally driven meridional circulation, analogous to tropospheric Hadley cell circulations. If we assume that the thermally driven circulation is small, we have $\partial\overline{T}_{\rm rad}/\partial t \approx -(\overline{T}_{\rm rad} - T_{\rm eq})/\tau_E$. The eddy-induced temperature $\overline{T}_{\rm dyn}$ follows:

$$\frac{\partial\overline{T}_{\rm dyn}}{\partial t} + \overline{w}^*\left(\frac{HN^2}{R}\right) = -\frac{\overline{T}_{\rm dyn}}{\tau_E}. \quad (3)$$

Integrating the equation from the time $t_0$ to $t$ yields

$$\overline{T}_{\rm dyn}(t) = e^{-(t-t_o)/\tau_E}\overline{T}_{\rm dyn}(t_o) - \frac{HN^2}{R}\int_{t_o}^{t} e^{-(t-s)/\tau_E}\overline{w}^*(s)\,ds. \quad (4)$$

This suggests that the dynamical cooling in the tropical stratosphere is the integrated consequence of the tropical upwelling prior to the cooling plus the decay of initial temperature anomaly. In the time mean, dynamical cooling is in balance with radiative heating.

An idealized atmospheric model and its zonally symmetric version are employed in sections 3–5 to study different branches of the residual circulation. Unlike the TEM form of Eq. (1), the models solve the Eulerian mean variables in the sigma coordinates (see the appendix for details). As such, we do not need to make the quasigeostrophic approximation as Eq. (1). This allows $T_{\rm rad}$ to differ from $T_{\rm eq}$ in the tropics to remove the effect of the thermally driven circulation from $T_{\rm dyn}$. More importantly, this allows us to diagnose the upwelling in the deep tropics, where the downward control calculation in Eq. (2) does not work because of small values of $\hat{f}$. As discussed above, the dynamical temperature change in the Eulerian mean equations can be used to diagnose the change in the residual circulation.

## 3. Model description and characteristics

We use the 1990s version of the Geophysical Fluid Dynamics Laboratory (GFDL) spectral atmosphere dynamical core (Gordon and Stern 1982). The model is forced by Newtonian relaxation toward prescribed zonally symmetric equilibrium temperature and damped by Rayleigh damping in the planetary boundary layer. To prevent inertial instability in the equatorial mesosphere, additional vertical diffusion is applied to the momentum and temperature equations as in Song and Robinson (2004). The model runs at rhomboidal 30 (R30) spherical harmonic truncations in the horizontal (approximately 3.75° lon × 2.25° lat) and 30 unevenly spaced sigma ($\sigma = p/p_s$) levels vertically [9 levels in the troposphere and 21 levels above the tropopause as in Scinocca and Haynes (1998)]. Similar mechanistic models have been used to study stratosphere–troposphere coupling (e.g., Taguchi et al. 2001; Polvani and Kushner 2002; Song and Robinson 2004; Gerber and Polvani 2009; Sun and Robinson 2009). Details of the model are documented in Sun et al. (2011) for a study of the downward influence of stratospheric final warming events, and here we briefly summarize the configuration for the stratospheric seasonal cycle and topographic forcing.

We fix the equilibrium temperature in the troposphere and impose a seasonal cycle above the nominal tropopause level of 100 hPa. The model is first spun up for 2000 days to reach a statistically steady state with stratospheric equilibrium temperature fixed for the perpetual NH winter solstice temperature, denoted by $T_{\rm winter}$. The next 800 days are branched every 10 days, and an 80-member ensemble is created by subjecting each realization to a seasonal transition of stratospheric equilibrium temperature for two consecutive years:

$$T_{\rm eq}(\phi, \sigma, t) = \gamma(t) \times T_{\rm winter}(\phi, \sigma) + [1 - \gamma(t)] \times T_{\rm summer}(\phi, \sigma), \quad (5)$$

where $\gamma(t) = 0.5 \times \{1 + \cos[2\pi \times t/(365\ \text{days})]\}$, and the perpetual NH summer solstice temperature is denoted by $T_{\rm summer}$. The SH equilibrium temperature is the mirror image of the NH temperature about the equator with a lag of 6 months. Since the equilibrium temperature in the troposphere is fixed, this experimental design allows us to isolate the impacts of the seasonal cycle of the stratosphere on the tropical upwelling.

To simulate different stratospheric seasonal cycles in the two hemispheres, a zonal wavenumber-1 surface topography is added in the NH (e.g., Taguchi et al. 2001):

$$h(\lambda, \phi) = 4h_0\mu^2(1 - \mu^2)\sin(m\lambda) \quad (\mu = \sin\phi,\ \mu \geq 0), \tag{6}$$

where $m$ is the zonal wavenumber, $\mu^2(1 - \mu^2)$ sets the mountain peak at $\phi = 45°$N, and $h_0$ controls the mountain height. Sun et al. (2011) explored the downward influence of stratospheric final warming with different mountain heights, zonal wavenumbers, polar vortex strengths, and horizontal resolution and found that the downward influences of stratospheric seasonal transition are qualitatively robust with model parameters. In this paper, we focus on the simulations with the topography $m = 1$ and $h_0 = 2$ km, which generates a realistic seasonal cycle of stratospheric circulation. In this configuration, the NH is dominated by stationary planetary waves, yet there are still transient planetary waves in the SH due to nonlinear interactions of baroclinic waves (Scinocca and Haynes 1998). This configuration is compared with the simulations where the topographic height $h_0$ is varied.

Additionally, a zonally symmetric model is used to evaluate the role of different wave forcings in driving the residual meridional circulation. The zonally symmetric model uses the same radiative forcing and dissipation as the full model, but only the zonal mean circulation is retained, and surface topography is then included in the eddy forcing. In this model, the eddy forcings are diagnosed from the daily output of the full model. This allows us to evaluate the residual circulation associated with different wavenumbers or different locations of the total eddy forcing. A detailed description of the zonally symmetric model and eddy forcings is given in the appendix.

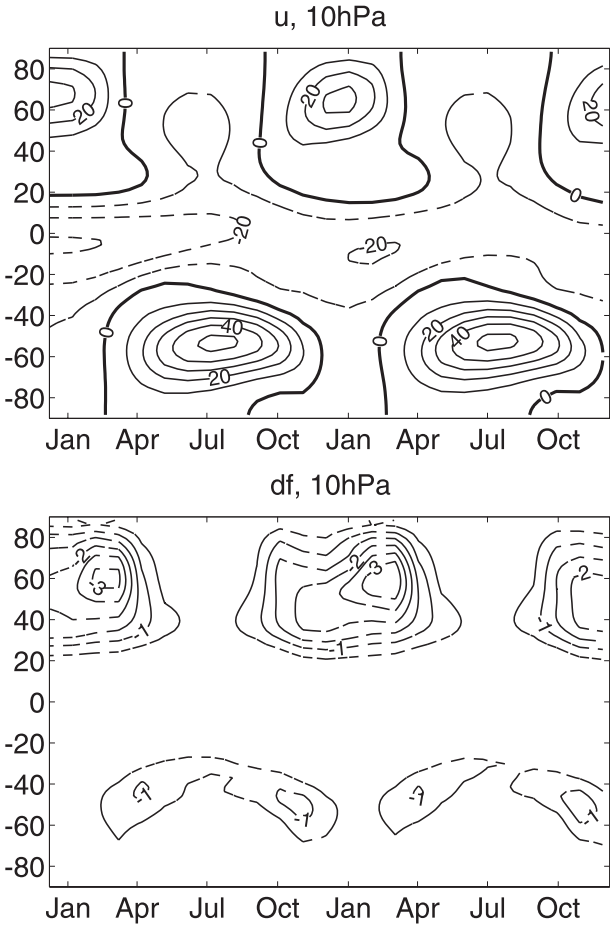


FIG. 1. Zonally, 30-day, and ensemble averaged (top) zonal wind and (bottom) EP flux divergence at 10 hPa in the full model in response to seasonally varying radiative heating. A 2-km zonal wavenumber-1 topography is imposed only in the NH. The ensemble mean is averaged over 80 realizations initialized from the NH winter solstice condition. The troposphere equilibrium temperature is set as equinoctial conditions to eliminate influences of the tropospheric seasonal cycle. The contour intervals are (top) 10 m $s^{-1}$ and (bottom) 0.5 m $s^{-1}$ $day^{-1}$.

## 4. Tropical stratospheric upwelling in the full model

In this section, we describe three aspects of the tropical upwelling in the stratosphere simulated in the full model. We first show that the model can simulate a reasonable annual cycle of tropical upwelling. Next, we highlight the nonlinearity of stratospheric waves to the strength of tropospheric planetary wave forcing. Finally, we contrast the roles of subtropical and high-latitude forcings in the seasonal and subseasonal variability.

### *a. Annual cycle*

Figure 1 shows zonally, 30-day, and 80-member-ensemble averaged zonal wind and the Eliassen–Palm (EP) flux divergence at 10 hPa simulated in the full model for 2 yr after the stratospheric equilibrium temperature is switched from the perpetual NH winter solstice temperature to a seasonal cycle in Eq. (5). In spite of the same midwinter radiative equilibrium temperature in the two hemispheres but with a lag of 6 months, the NH planetary wave drag (EP flux convergence) is stronger and the polar night jet is weaker than their SH counterparts. The SH wave drag maximizes during the fall and during the spring with a midwinter minimum, while the NH wave drag maximizes near midwinter, which can be qualitatively explained by the Charney–Drazin criterion for planetary wave propagation (Charney and Drazin 1961) and different stratospheric wave–mean flow interactions in the two hemispheres (Plumb 1989; Scott and Haynes

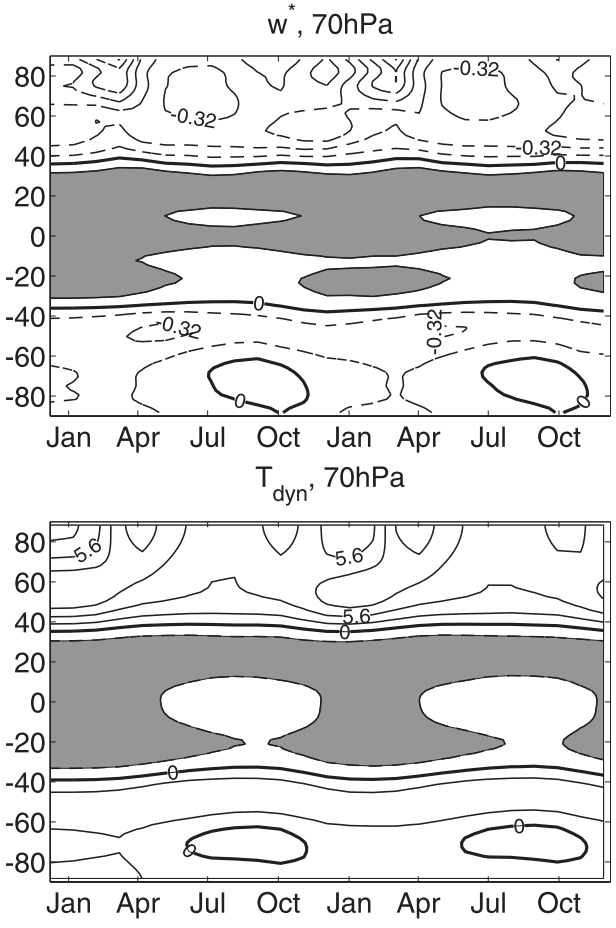


FIG. 2. Zonally, 30-day, and ensemble averaged (top) residual vertical velocity and (bottom) eddy-induced temperature at 70 hPa in the full model in response to seasonal radiative heating. The eddy-induced temperature is defined as the deviation from the temperature in the eddy-free simulation under the same radiative equilibrium temperature change. The ensemble mean is averaged over 80 realizations. The contour intervals are (top) 0.16 mm $s^{-1}$ and (bottom) 2.8 K, respectively.

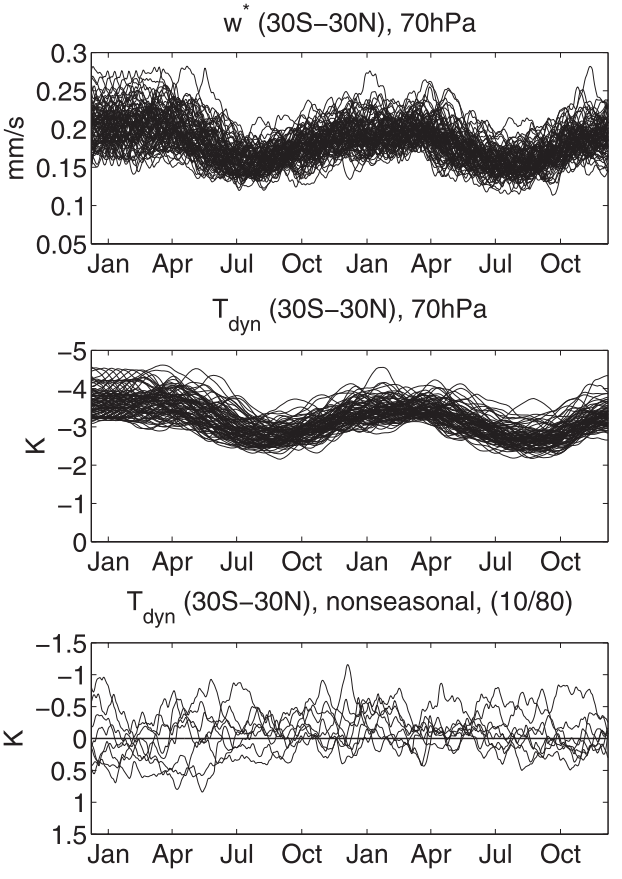


FIG. 3. Zonally and 30-day averaged (top) residual vertical velocity and (middle) eddy-induced temperature at 70 hPa and in the tropics (30°S–30°N) in the full model in response to seasonal radiative heating. (bottom) Subseasonal daily temperature variation for 10 out of 80 realizations after removing the 80-member-ensemble mean annual cycle. Note that the vertical axis of temperature variability is reversed to highlight tropical cooling/upwelling.

2002; Yoden et al. 2002; Plumb 2010). Despite the simplicity of our model, the model can simulate the major characteristics of observed stratospheric seasonal cycles in the two hemispheres (e.g., Randel 1988).

The model can simulate a reasonable annual cycle of the residual circulation in the lower stratosphere. The zonally averaged residual vertical velocity and eddy-induced temperature at 70 hPa are displayed in Fig. 2. The residual circulation rises in the tropics and descends in the extratropics with the zero crossing latitudes at about 30°N/S, and the strength of the BDC is stronger during January than during July. This resembles the seasonal cycle of the residual circulation in the observations (e.g., Randel et al. 2008; Ueyama and Wallace 2010). The ensemble mean upwelling (downwelling) and dynamic cooling (warming) are anticorrelated throughout the annual cycle. A similar seasonal change in the eddy-induced temperature is seen in the middle and upper stratosphere, and the seasonal cycle attenuates downward into the troposphere (not shown) because of fixed tropospheric equilibrium temperature. As there is no seasonal change in the equilibrium temperature below 100 hPa, this demonstrates that the seasonal cycle of the stratosphere alone can lead to a seasonal cycle in the tropical stratospheric upwelling.

Individual realizations throughout the seasonal cycle are shown for the zonally averaged tropical (30°S–30°N) upwelling and dynamical cooling at 70 hPa. The top two panels of Fig. 3 show that individual realizations, smoothed by a 30-day running mean, undergo a clear seasonal cycle with a correlation of 0.83 between the upwelling and dynamical cooling, consistent with Eq. (3). After removing the 80-member-ensemble mean annual cycle in the dynamical cooling, the remaining unsmoothed data exhibit

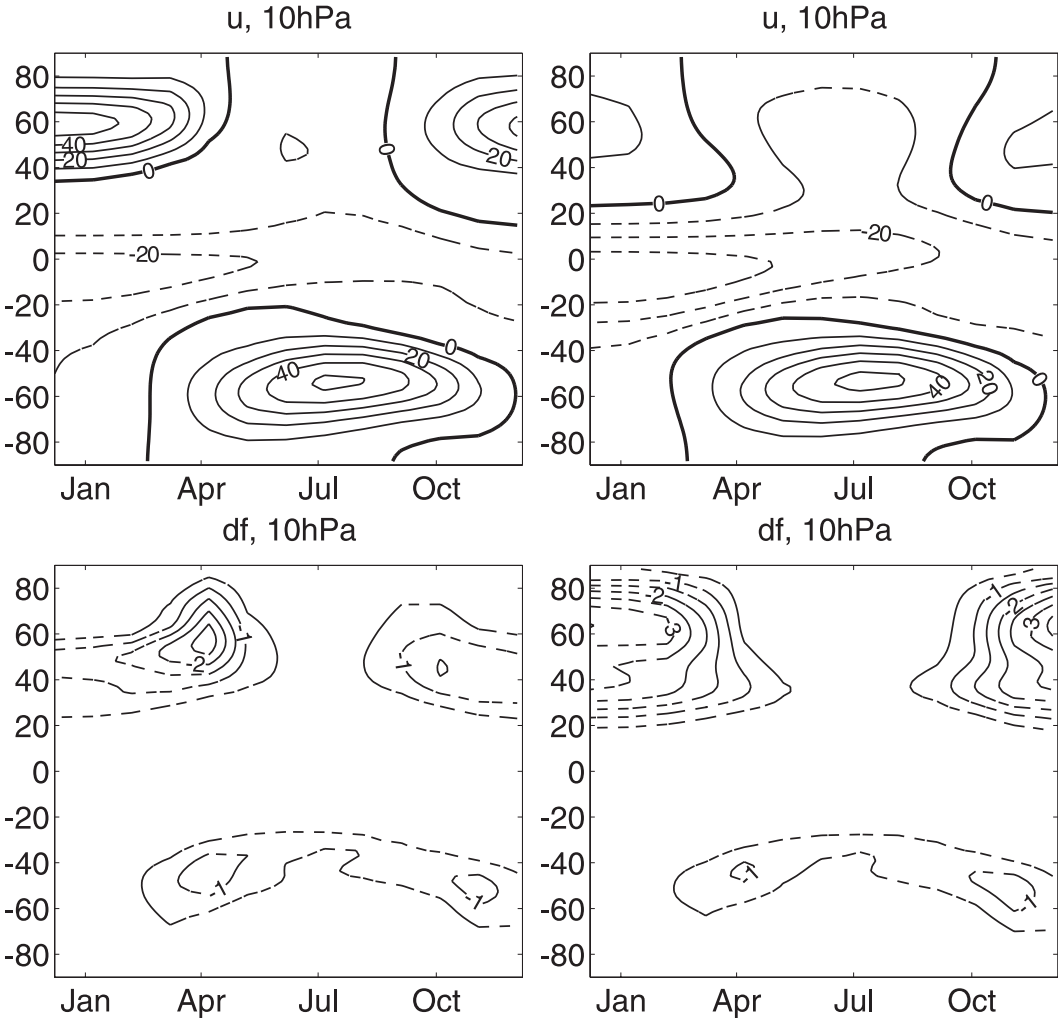


FIG. 4. As in Fig. 1, but for the zonally, 30-day, and ensemble averaged (top) zonal wind and (bottom) EP flux divergence at 10 hPa in the full model with (left) 1- and (right) 3-km topography. Note that only the first year ensemble mean is shown, in contrast to the first 2-yr ensemble mean shown in Fig. 1.

considerable subseasonal variability, as in the observations (e.g., Randel et al. 2002a). The instantaneous correlation between the subseasonal daily tropical upwelling and dynamical cooling is reduced to 0.43, as expected from Eq. (4), but the correlation is still statistically significant. This confirms the dynamical balance between tropical upwelling and radiative heating in the lower stratosphere as described in section 2.

### b. *Sensitivity to the strength of the planetary wave forcing*

The strength of planetary wave forcing can affect the seasonal cycle of tropical upwelling in different ways. The middle-atmosphere Hadley cell circulations may respond nonlinearly to the amplitude of the wave drag, especially when the drag is strong (Scott and Haynes 2002; Zhou et al. 2006). Also, the strength of the planetary wave forcing can control the timing of maximum wave drag, as is the case for the difference between the two hemispheres (Fig. 1), which can, in turn, affect the seasonal evolution of tropical upwelling.

Figure 4 shows zonally and 80-member-ensemble averaged zonal wind and the EP flux divergence at 10 hPa as in Fig. 1, but $h_0$ in the NH is changed from 2 to 1 and 3 km, respectively. Given the resemblance between the first year and the second year ensemble means in Fig. 1, only the first year is shown here. In comparison with Fig. 1, as the NH topographic forcing is reduced to the 1-km mountain height, the simulated zonal wind in the NH is stronger and the wave drag maximum is delayed to the boreal spring. Conversely, as the forcing is increased to the 3-km mountain height, the NH polar vortex is more

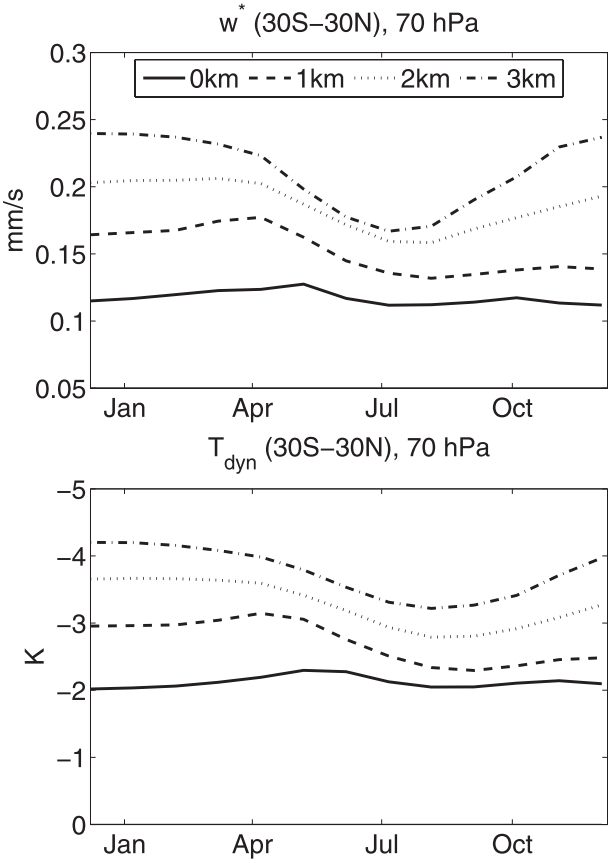


FIG. 5. The zonally, 30-day, and ensemble averaged (top) residual vertical velocity and (bottom) eddy-induced temperature at 70 hPa and in the tropics (30°S–30°N) in the full model for different mountain heights. Note that the vertical axis of temperature variability is reversed to highlight tropical upwelling/cooling.

disturbed during midwinter. This is consistent with the nonlinear behaviors of planetary waves with regard to the amplitude of surface forcing in mechanistic models of the stratosphere (Plumb 1989; Scott and Haynes 2002; Yoden et al. 2002; Plumb 2010).

The change in the seasonal cycle of the wave drag can further influence the evolution of tropical upwelling. Figure 5 compares the seasonal cycle of zonally and ensemble averaged tropical upwelling and dynamical cooling for the mountain heights of 0, 1, 2, and 3 km. In the absence of the NH topographic forcing, there is no distinct seasonal cycle in the tropical upwelling, although there still exists a weak seasonal cycle of planetary waves (see the SH of Fig. 4). As the mountain height is increased gradually, a peak of tropical upwelling first appears during the NH spring under weak forcing (1-km mountain) and then shifts to the NH midwinter under strong forcing (3-km mountain), in accordance with the change of wave drag in Fig. 4. This suggests that the maximum tropical upwelling during January is primarily driven by the NH planetary wave forcing.

### c. Seasonal and subseasonal variability

As discussed in the introduction, the meridional extent in the residual circulation response to prescribed wave drag depends on the ratio of the time scales of the wave drag and the radiative damping (Haynes et al. 1991; Holton et al. 1995). Our model uses the radiative damping rate of Holton and Mass (1976), which varies from about 23 days near 100 hPa to about 5 days near 1 hPa. Therefore, the meridional extent of the residual circulation response to a wave drag may differ for the seasonal and subseasonal variability.

We first define an index of tropical upwelling as the zonally averaged daily eddy-driven temperature at 70 hPa and between 30°S and 30°N, and the index is normalized and inverted to represent tropical cooling/upwelling in a regression analysis. Figure 6 shows the regression of the EP flux divergence at 10 hPa onto the indices of tropical upwelling. The EP flux divergence associated with the total variability of tropical upwelling is preceded by strong wave drag in the NH with a maximum at about −45-day lag, and weak wave drag in the SH with a maximum at about −20-day lag. This is consistent with different annual cycles of the wave drag in the two hemispheres in Fig. 1. After removing the ensemble mean annual cycle in the upwelling index, the EP flux divergence associated with the subseasonal variability is roughly of equal amplitude in the two hemispheres with the maximum at about −15-day lag. This confirms that the persistence of the wave drag is larger for the seasonal variability in tropical upwelling than for the subseasonal variability, especially in the NH.

Next, we compare the vertical regression patterns of the EP flux divergence at the time of maximum correlation with the eddy-induced temperature at the zero lag (Fig. 7). The model again simulates the features of stratospheric temperature variability in the observations (e.g., Ueyama and Wallace 2010): the amplitude of tropical dynamical cooling is greater in the seasonal variability than in the subseasonal variability, and the hemispherically averaged BDC at both time scales is characterized as tropical cooling and high-latitude warming with a change in sign at about 45°N/S. The variability of EP flux convergence in the stratosphere at both time scales is associated with the change in the troposphere.

However, the seasonal and subseasonal variabilities of tropical upwelling display somewhat different characteristics. On the subseasonal time scale (the right panel of Fig. 7), the regression patterns of wave drag in the two hemispheres are fairly symmetric about the equator, and therefore the wave forcings in both hemispheres are

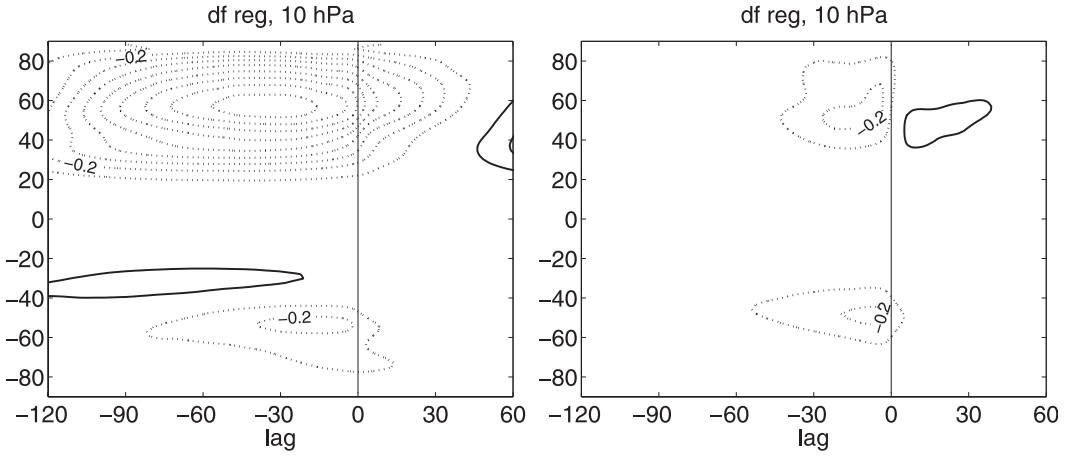


FIG. 6. The lagged regression of the EP flux divergence at 10 hPa onto the indices of (left) total and (right) subseasonal variability in tropical upwelling. The index of the tropical upwelling is defined as the zonally averaged daily eddy-driven temperature at 70 hPa and between 30°S and 30°N, and the index is normalized and inverted to represent tropical cooling/upwelling. The subseasonal variability is the residual after removing the ensemble mean annual cycle. The contour interval is 0.1 m $s^{-1}$ $day^{-1}$.

likely to contribute to the tropical cooling. This is consistent with the view that transient wave drag in high latitudes is sufficient to drive upwelling (e.g., Holton et al. 1995).

On the seasonal time scale (the left panel of Fig. 7), the NH wave drag is much larger and occurs above 30 hPa, while the SH drag is smaller and concentrates around 30 hPa. As the residual vertical velocity is the consequence

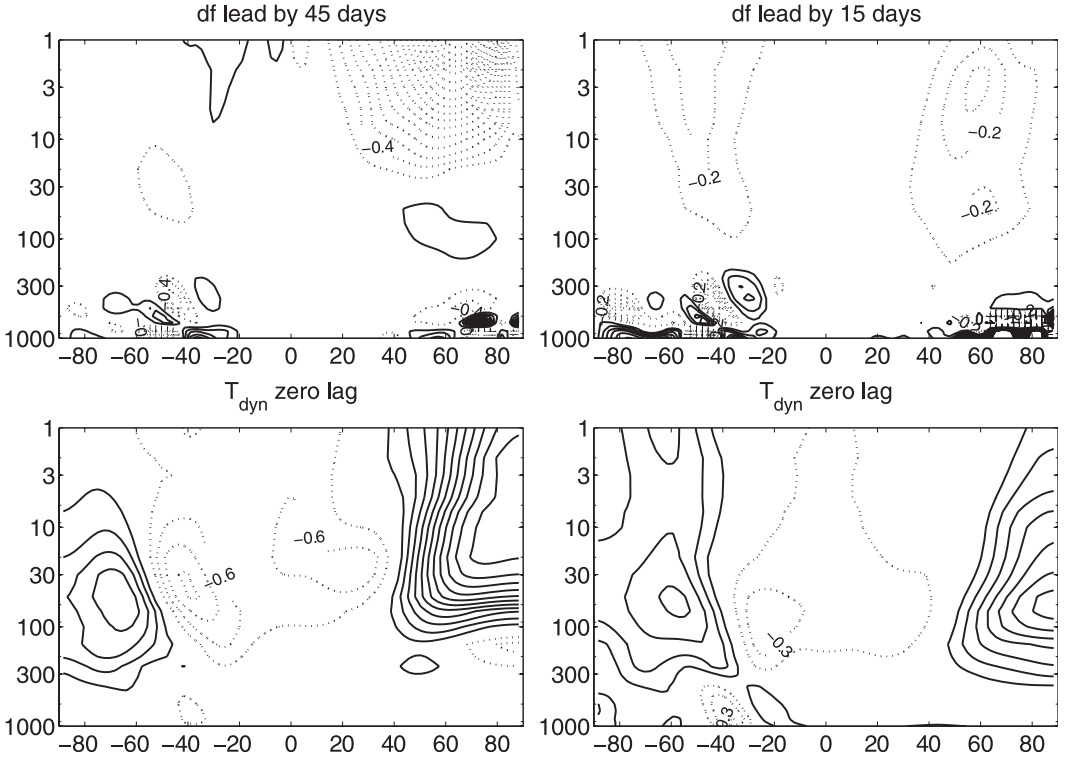


FIG. 7. The lagged regression of the (top) EP flux divergence and (bottom) eddy-induced temperature onto the indices of (left) total and (right) subseasonal variability in tropical upwelling. The indices of tropical upwelling are defined as in Fig. 6. The contour intervals are (top left) 0.2 m $s^{-1}$ $day^{-1}$, (top right) 0.1 m $s^{-1}$ $day^{-1}$, (bottom left) 0.3 K, and (bottom right) 0.15 K.

of the mass-weighted integral of wave drag above the level of interest [Eq. (2)], the temperature regression patterns in the two hemispheres are comparable in amplitude. Nevertheless, the NH wave drag and associated tropical cooling extend more deeply into the tropics than their SH counterparts. For example, the zero-crossing latitudes of eddy-driven temperature in the NH (about 30°–40°N at 100–30 hPa) is more equatorward than the zero-crossing latitudes in the SH (about 45°–55°S at 100–30 hPa). Consequently, the dynamical cooling at the equator appears to be more related to the upwelling in the NH, and the cooling in the SH is more confined in the subtropical latitudes. It is further demonstrated in section 5 (Fig. 10d) that the wave drag in the NH contributes most to the tropical cooling. As such, the hemispheric asymmetry is consistent with the notion that persistent wave drag needs to extend to the subtropics to drive sufficient tropical upwelling. It also suggests that hemispherically asymmetric wave drag can lead to hemispherically more-symmetric tropical cooling, possibly through nonlinear tropical dynamics, analogous to tropospheric Hadley cell circulations (e.g., Plumb and Eluszkiewicz 1999).

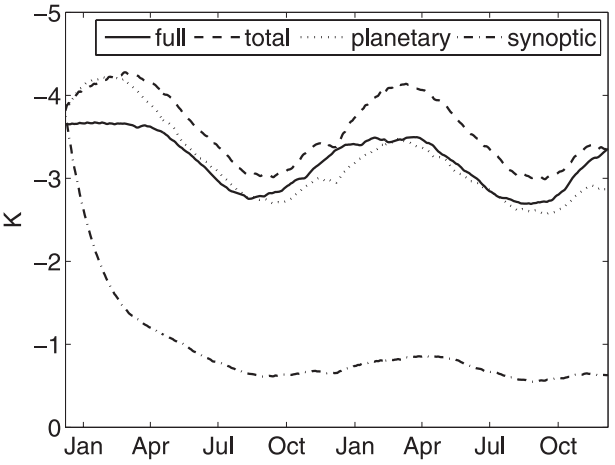


FIG. 8. The zonal mean eddy-induced temperature at 70 hPa and in the tropics (30°S–30°N) in response to prescribed eddy forcings and seasonal radiative heating in a zonally symmetric model. The planetary wave (wavenumbers 1–3), synoptic wave (wavenumbers 4 and above), and total eddy forcings are calculated from the full model with seasonal radiative heating.

## 5. Dynamics of tropical upwelling in a zonally symmetric model

Following the full model results in section 4, the dynamics of the seasonal variability in tropical upwelling is probed with a zonally symmetric version of the full model. We first test to what extent the seasonal cycle of tropical upwelling can be reproduced by imposing the ensemble mean daily eddy forcings from the full model and seasonally varying radiative heating. Next, we run the model with the perpetual NH winter solstice condition. The zonally symmetric model is utilized to separate the dynamical response due to different wavenumbers or different locations of the total eddy forcing.

Figure 8 shows the zonal mean eddy-induced temperature in the tropical lower stratosphere in response to the total or partial eddy forcing diagnosed from the full model as well as the same seasonal change in the equilibrium temperature. The total eddy forcing is separated between planetary-scale waves (wavenumbers 1–3) and synoptic-scale waves (wavenumbers 4 and above). In comparison with the full model, both the total and planetary wave forcings can approximately reproduce the seasonal cycle of tropical upwelling, although the seasonal cycle in the zonally symmetric model is somewhat delayed in time. By contrast, the tropical upwelling in response to the synoptic wave forcing decays rapidly from the initial conditions. Note that the sum of the responses to synoptic eddies plus planetary eddies is not equal to the response to the total forcing initially because of influences of initial conditions [Eq. (4)]. This suggests that not only the seasonal cycle but also the climatological mean of the lower stratospheric upwelling is primarily caused by the planetary wave forcing.

The vertical structures of zonal mean temperature changes in the full model and in the zonally symmetric model are displayed for the total, planetary, and synoptic wave forcings (Fig. 9). We focus on the month of January in the second year ensemble mean when the upwelling is strongest and the influences from initial conditions are negligible. In the full model, the residual vertical circulation rises in the tropics and, interestingly, the width of the rising region broadens from about 20°N/S at 200 hPa to 40°N/S at 30 hPa. The subsidence takes place throughout the winter extratropical stratosphere and is confined to the summer extratropical lower stratosphere. The latter is due to the predominant easterly winds that prevent the deep propagation of planetary waves. Similar eddy-induced temperature is found during July (not shown), except that the descent in the winter hemisphere occurs only in the middle latitudes because of a strong SH polar vortex that prevents the subsidence into the interior of the polar vortex (e.g., Fig. 2 in Plumb 2002).

Figure 9 shows that the full model eddy-induced temperature change is well reproduced by the zonally symmetric model. As the total eddy forcing is separated by planetary waves and synoptic waves, the planetary wave forcing drives tropical cooling and high-latitude warming extending from the stratosphere downward to the surface, while the synoptic wave forcing drives the tropical upwelling and midlatitude downwelling in the troposphere. These patterns are consistent with stratospheric

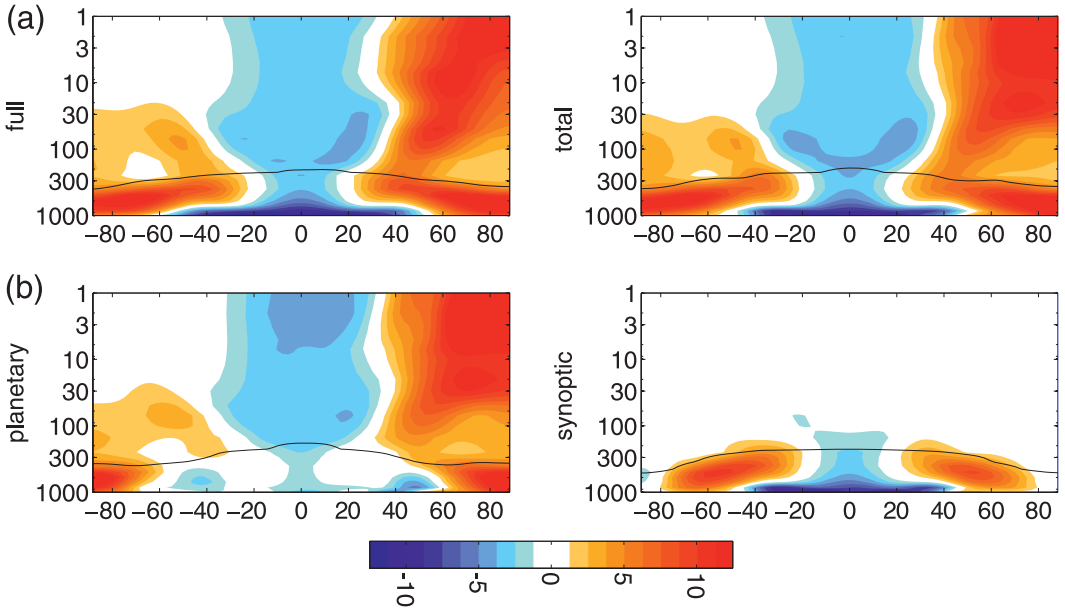


FIG. 9. The eddy-induced temperature change during January of the second year in Fig. 8 in the full model and in the zonally symmetric model with the total, planetary, and synoptic eddy forcings diagnosed from the full model. The black line indicates the tropopause level in each simulation determined by the World Meteorological Organization (WMO) lapse rate definition.

and tropospheric residual circulations in the observations (e.g., Edmon et al. 1980; Rosenlof 1995). One should note that the same eddy-induced temperature anomaly implies greater residual vertical velocity in the troposphere than in the stratosphere for the smaller tropospheric static stability and relaxation time scale; that is, in the steady state, Eq. (3) yields $\overline{w}^* = -(\overline{T}_{\rm dyn}R)/(HN^2\tau_E)$.

The responses to planetary and synoptic wave forcings are approximately additive except in the tropical upper stratosphere. As a first-order approximation, the planetary wave forcing contributes most to the residual circulation in the stratosphere and the high-latitude troposphere, and the synoptic wave forcing dominates the residual circulation in the tropical and midlatitude troposphere. Both of them contribute to the residual circulation in the lowermost stratosphere. Because the tropical stratospheric zonal wind under partial eddy forcings differs considerably from the full model, the decomposition also suggests that the seasonal change of zonal wind and nonlinear middle-atmosphere Hadley circulations in Eq. (1) are secondary to the wave drag except in the tropical upper stratosphere. Therefore, we further explore the sensitivities of the residual circulation to different components of the wave drag.

The total eddy forcing is separated by four different pairs of decomposition in wavenumber or in region under the perpetual NH winter solstice condition (Fig. 10). As in Fig. 9b, the planetary wave forcing accounts for the stratospheric tropical upwelling and extratropical downwelling into the high-latitude troposphere, and the synoptic wave forcing accounts for the tropospheric tropical upwelling and midlatitude downwelling in the troposphere (Fig. 10b). This is remarkably similar to the temperature response to the stratospheric forcing and tropospheric forcing, which separate the total forcing by the nominal tropopause level (100 hPa), except in the high-latitude troposphere (Fig. 10c). Interestingly, the temperature response to stratospheric forcing also suggests that stratospheric dynamics can have a large impact on global tropopause structure (e.g., Thuburn and Craig 2000; Kirk-Davidoff and Lindzen 2000). Next, as discussed in section 4c, the total forcing is divided into the NH and SH forcings by the equator. While the NH eddy forcing explains most of the tropical stratospheric upwelling, the SH wave drag can only induce subtropical upwelling and even induce equatorial downwelling in the stratosphere (Fig. 10d). Finally, as the total forcing is divided into the tropical and extratropical forcings by 30°S/N (approximately the mean zero-crossing latitude in the lower stratosphere in Fig. 10a), most of the lower stratospheric upwelling is caused locally by the tropical wave drag, and the extratropical wave drag can only induce upwelling in the subtropics (Fig. 10e).

Figures 10b–e suggest that the tropical upwelling in this model can be mostly attributed to the planetary wave forcing in the winter tropical and subtropical stratosphere.

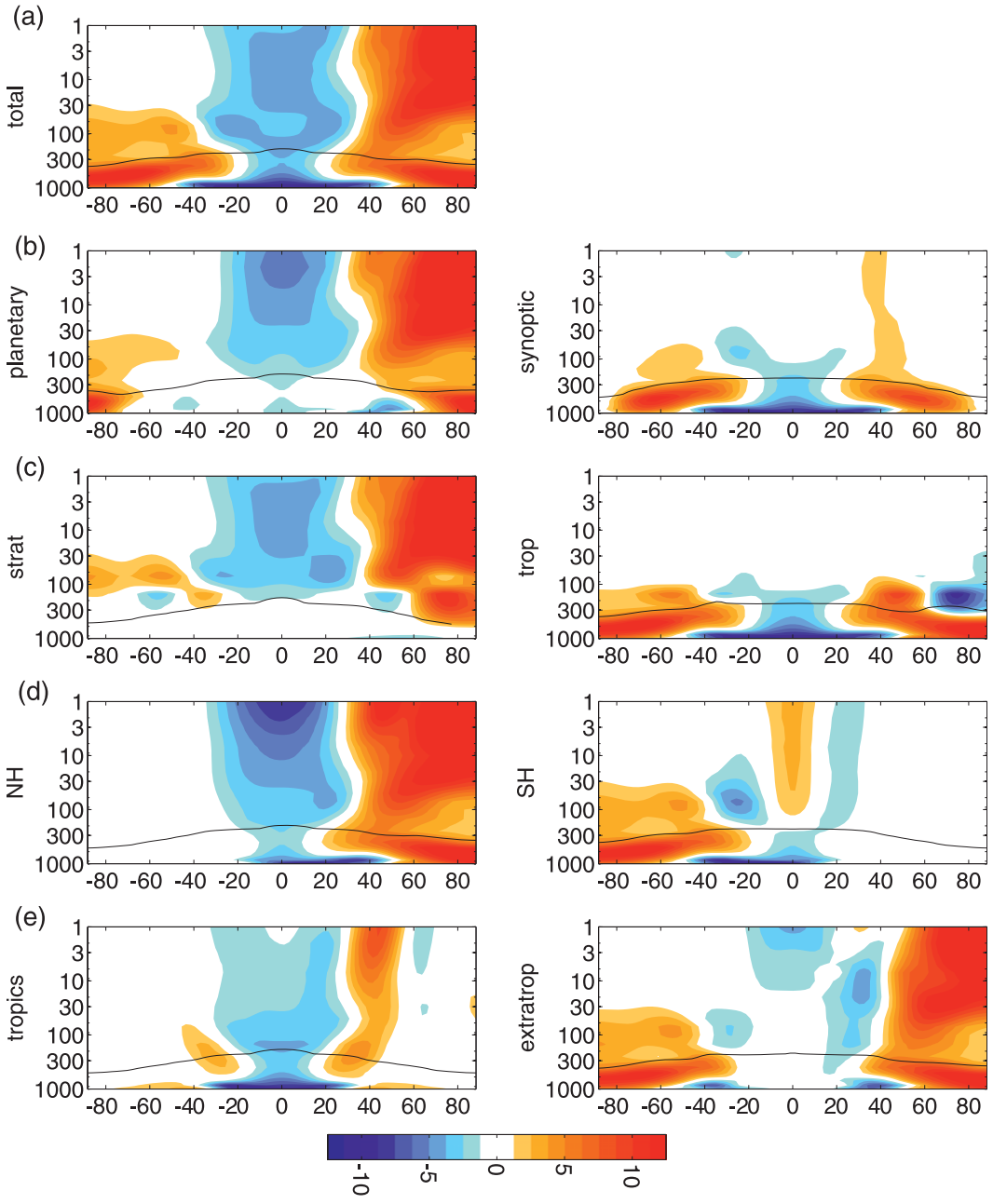


FIG. 10. The eddy-induced temperature change in the zonally symmetric model with the eddy forcings from the full model under the perpetual NH winter solstice condition. The total forcing is compared with four different pairs of decomposition: (a) total eddy forcing, (b) planetary wave forcing vs synoptic wave forcing, (c) stratospheric forcing vs tropospheric forcing (separated by the nominal tropopause level of 100 hPa), and (d) tropical forcing vs extratropical forcing (separated by 30°S/N). The black line indicates the actual tropopause level in each simulation determined by the WMO lapse rate definition.

Since the topographic forcing is imposed mainly in the extratropics, planetary waves have to propagate equatorward to the subtropical latitudes to induce sufficient upwelling (e.g., Plumb and Eluszkiewicz 1999). The equatorward propagation is confirmed by an additional experiment that separates the total forcing by the eddy momentum flux and heat flux forcings (not shown). This experiment shows that the tropical and subtropical eddy momentum flux divergence is more important for the tropical stratospheric upwelling, and that the extratropical

eddy heat flux contributes most for the high-latitude warming in the stratosphere.

In comparison with different components of the residual circulation depicted in Fig. 2 of Plumb (2002), in addition to the synoptic component in the summer lower stratosphere, Figs. 9b and 10b indicate one additional branch of residual circulation due to planetary waves, which ascends in the subtropics and descends in the extratropics. These planetary waves can arise from nonlinear interactions of baroclinic waves (Scinocca and Haynes 1998), and the waves are possible because the zero wind line remains around 50 hPa in the summer. The planetary wave forcing and associated nonlinear isentropic mixing may serve as an important pathway for the dynamical transport in the summer lower stratosphere (e.g., Birner and Bönisch 2010).

## 6. Conclusions and discussion

The role of extratropical waves in the tropical upwelling branch of the Brewer–Dobson circulation is investigated in an idealized model of the stratosphere and troposphere. Seasonally varying radiative heating is imposed only in the stratosphere to eliminate influences of the tropospheric seasonal cycle. Surface topographic forcing is prescribed only in the NH to simulate different stratospheric eddy–mean flow interactions in the two hemispheres. A zonally symmetric version of the same model is used to diagnose the effects of different wavenumbers and different regions of the total forcing on the tropical stratospheric upwelling.

Despite its simplicity, the model can simulate a reasonable seasonal cycle in the tropical upwelling in the lower stratosphere with a stronger amplitude during January (NH winter) than during July (NH summer), corroborating the importance of stratospheric planetary waves in the observed seasonal cycle of tropical upwelling. As in the mechanistic models of the stratosphere (e.g., Holton and Mass 1976; Plumb 1989; Scott and Haynes 2002; Yoden et al. 2002; Plumb 2010), the seasonal cycle of stratospheric planetary waves responds nonlinearly to the strength of the tropospheric forcing, which maximizes during midwinter for the strong NH-like planetary forcing but maximizes during the fall and spring for the weak SH-like forcing. Using a zonally symmetric version of the full model, the planetary wave component of the total forcing can approximately reproduce the seasonal cycle of tropical stratospheric upwelling.

The temperature response to the eddy forcing during the NH winter solstice displays a pattern of tropical cooling and extratropical warming with the zero-crossing latitudes at 30°–40°N and 45°–55°S. The planetary wave forcing contributes most to the residual circulation in the stratosphere and in the high-latitude troposphere, and the synoptic wave forcing dominates the residual circulation in the tropical and midlatitude troposphere. As the total forcing is decomposed into different wavenumbers or different regions, it is found that the planetary wave forcing in the winter tropical and subtropical stratosphere contributes most to the tropical stratospheric upwelling. This suggests that the planetary wave forcing, prescribed mostly in the extratropics in the model, has to propagate equatorward into the subtropical latitudes to induce sufficient tropical upwelling, consistent with the mechanistic models of the stratosphere (Plumb and Eluszkiewicz 1999; Semeniuk and Shepherd 2001a; Scott 2002; Zhou et al. 2006; Geller et al. 2008). Therefore, the tropical and subtropical wave drag is more important for the seasonal cycle of tropical stratospheric upwelling than the high-latitude forcing, while the high-latitude forcing may remain to play an important role for the subseasonal variability of the tropical upwelling (cf. Figs. 7 and 10d).

Although the tropospheric equilibrium temperature and surface topography are fixed in our model, the observed tropospheric wave forcing in the NH undergoes a distinct seasonal cycle, and is greatest during the wintertime due to strongest land–sea contrasts and associated diabatic heating (Wang and Ting 1999). The seasonal cycle of stratospheric waves is, however, more constrained by the lower stratospheric waveguide (e.g., Chen and Robinson 1992) and the influence of tropospheric seasonal cycle would likely be secondary. To test this, we have performed a set of experiments with a seasonal cycle in both the stratosphere and the troposphere. The tropospheric seasonal cycle is realized through varying the parameter for hemispherically asymmetric heating in Polvani and Kushner (2002) from $\epsilon = 10$ K during the winter to $-10$ K during the summer. Figure 11 shows the seasonal cycle of residual vertical velocity and eddy-induced temperature at 70 hPa. This is very similar to the case without a tropospheric seasonal cycle in Fig. 2. With the tropospheric seasonal cycle, the warming in the polar vortex is greater, and this can be attributed to a stronger tropospheric subtropical jet that supports more upward wave propagation into the polar vortex. The tropospheric seasonal cycle has a larger impact on the tropical upwelling as one moves from 70 to 100 hPa. This can be expected from Fig. 9b, which shows a larger influence of synoptic waves on the tropical cooling at 100 hPa than at 70 hPa. In the observations, Randel et al. (2008) also showed possible influences of extratropical synoptic eddies on the tropical upwelling at 100 hPa.

In comparison with the paradigms of the residual circulation depicted in Plumb (2002), Figs. 9b and 10d suggest that planetary waves in the summer lower stratosphere can drive a branch of the residual circulation rising in the

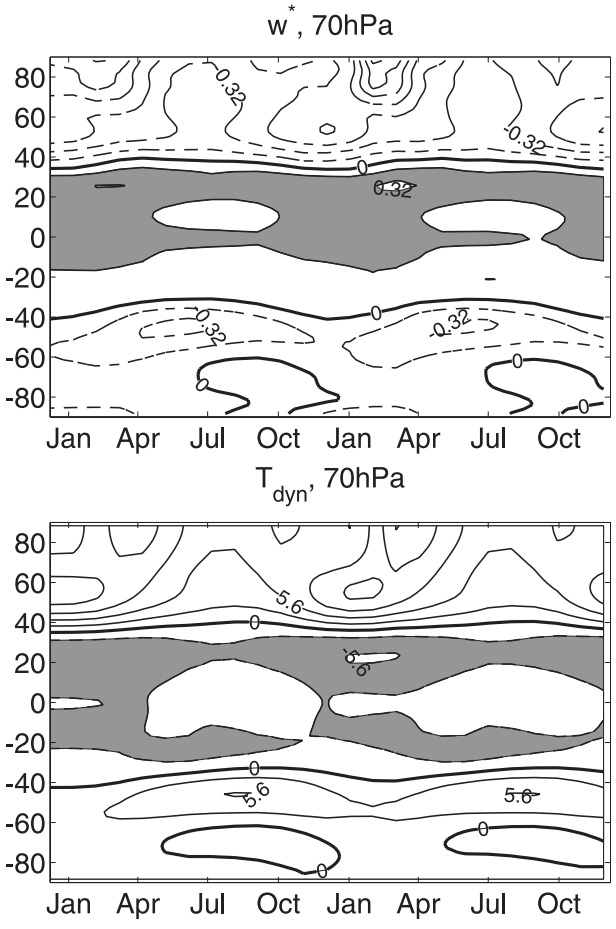


FIG. 11. As in Fig. 2, but for the seasonal cycle in both the stratosphere and the troposphere. The tropospheric seasonal cycle is realized through varying the parameter for hemispherically asymmetric heating in Polvani and Kushner (2002) from $\epsilon = 10$ K during the winter to $-10$ K during the summer. The ensemble mean is averaged over 80 realizations. The contour intervals are (top) 0.16 mm s$^{-1}$ and (bottom) 2.8 K, respectively.

subtropics and sinking in the extratropics. These waves are possible because the zero wind line remains around 50 hPa during the summer. This shallow residual circulation may be an important pathway for the dynamical transport in the summer lower stratosphere (e.g., Birner and Bönisch 2010). Also, we have not explored in this study the possible roles of tropical stationary waves, tropical convection, or monsoon circulations (e.g., Kerr-Munslow and Norton 2006; Randel et al. 2008; Taguchi 2009) and parameterized gravity waves (e.g., Randel et al. 2008; Li et al. 2008; McLandress and Shepherd 2009) in the tropical stratospheric upwelling. These issues are currently investigated in similar idealized models.

*Acknowledgments.* We are greatly thankful for discussions with Rei Ueyama, Mike Wallace, Alan Plumb, Peter Hess, and Steve Colucci. We thank two anonymous reviewers for constructive comments on our manuscript. GC and LS are supported by a startup fund from Cornell University, and GC is partially supported by the National Science Foundation (NSF) Climate and Large-Scale Dynamics program under Grant AGS-1042787.

## APPENDIX

### Zonally Symmetric Model

The zonal symmetric model is derived from the full model and only zonal mean components of the vorticity, divergence, temperature, and the natural logarithm of the surface pressure are integrated every time step. In the zonally symmetric model, the eddy forcing in the meridional momentum equation can be neglected and we only consider the eddy forcing for the zonal wind, temperature, and logarithm surface pressure equations, represented by $F_u$, $F_T$, and $F_{\ln P_s}$, respectively.

The zonally symmetric model equations are

$$\frac{\partial \overline{u}}{\partial t} + \overline{v}\left[\frac{1}{a\cos\phi}\frac{\partial(\overline{u}\cos\phi)}{\partial\phi} - f\right] + \overline{\dot{\sigma}}\frac{\partial \overline{u}}{\partial\sigma} = F_u, \tag{A1}$$

$$\frac{\partial \overline{T}}{\partial t} + \frac{\overline{v}}{a}\frac{\partial \overline{T}}{\partial\phi} + \overline{\dot{\sigma}}\frac{\partial \overline{T}}{\partial\sigma} - \kappa\overline{T}\overline{\left(\frac{\omega}{p}\right)} = F_T, \tag{A2}$$

$$\frac{\partial \overline{\ln(P_s)}}{\partial t} + \frac{\overline{v}}{a}\frac{\partial \overline{\ln(P_s)}}{\partial\phi} + \widetilde{D} = F_{\ln P_s}, \quad \text{and} \tag{A3}$$

$$\frac{\partial \overline{\dot{\sigma}}}{\partial\sigma} + \frac{\overline{v} - \widetilde{\overline{v}}}{a}\frac{\partial \overline{\ln(P_s)}}{\partial\phi} + (\overline{D} - \widetilde{\overline{D}}) = 0, \tag{A4}$$

where the overbar and tildes represent zonal and vertical averages, respectively; the prime means the deviation from the zonal mean; $a$ is the radius of the earth; $f$ is the Coriolis parameter; $R$ is the gas constant for dry air; $\kappa$ is the ratio of gas constant to specific heating at constant pressure; $u$, $v$, $D$, $T$, and $P_s$ are the zonal wind, meridional wind, divergence, temperature, and surface pressure; $\dot{\sigma}$ and $\omega$ are the vertical velocity in the sigma and pressure coordinates; $p$ is the pressure associated with the sigma level ($p = P_s\sigma$); and $\phi$ is the latitude. The eddy forcings are

$$F_u = \frac{1}{\overline{P_s}}\left\{-\frac{1}{a\cos^2\phi}\frac{[\overline{\partial(P_s v)'u'}\cos^2\phi]}{\partial\phi} - \frac{\overline{\partial(P_s\dot{\sigma})'u'}}{\partial\sigma} - \frac{1}{a\cos\phi}\overline{P_s'\frac{\partial(\Phi - RT)'}{\partial\lambda}} + C_u\right\}, \tag{A5}$$

$$F_T = \frac{1}{\overline{P_s}}\left\{-\frac{1}{a\cos\phi}\frac{\partial[\overline{(P_s v)'T'}\cos\phi]}{\partial\phi} - \frac{\partial\overline{(P_s\dot{\sigma})'T'}}{\partial\sigma} + C_{T1} + C_{T2}\right\}, \quad \text{and} \tag{A6}$$

$$F_{\ln P_s} = -\overline{\tilde{\mathbf{v}}' \cdot \nabla[\ln(P_s)]'}, \tag{A7}$$

where $\lambda$ is the longitude, $\Phi$ is the geopotential height, and $\mathbf{v}$ is the horizontal wind vector with components $u$ and $v$. The first three terms in Eq. (A5) are meridional momentum flux, vertical momentum flux, and form drag. The first two terms in Eq. (A6) are meridional heat flux and vertical heat flux; $F_{\ln P_s}$, $G_u$, $G_{T1}$, and $G_{T2}$ are the corrections to the zonally symmetric model by considering the extra covariances in the full model. Also,

$$C_u = -\overline{P_s' v'}\left[\frac{1}{a\cos\phi}\frac{\partial(\overline{u}\cos\phi)}{\partial\phi} - f\right] - (\overline{P_s'\dot{\sigma}'} + \overline{P_s}\delta\overline{\dot{\sigma}})\frac{\partial\overline{u}}{\partial\sigma}, \tag{A8}$$

$$C_{T_1} = -\frac{\overline{P_s' v'}}{a}\frac{\partial\overline{T}}{\partial\phi} - (\overline{P_s'\dot{\sigma}'} + \overline{P_s}\delta\overline{\dot{\sigma}})\frac{\partial\overline{T}}{\partial\sigma}, \quad \text{and} \tag{A9}$$

$$C_{T_2} = \kappa\cdot\left[\overline{P_s\frac{\omega}{p}T} - \overline{P_s}\,\overline{\left(\frac{\omega}{p}\right)}\,\overline{T}\right], \tag{A10}$$

where $\delta\overline{\dot{\sigma}}$ is the correction to the diagnosed sigma vertical velocity in the zonally symmetric model and can be obtained by

$$\frac{\partial(\delta\overline{\dot{\sigma}})}{\partial\sigma} = -\overline{(v - \tilde{v})' \cdot \nabla[\ln(P_s)]'}. \tag{A11}$$

In practice, before the zonally symmetric run, $F_u$, $F_T$, and $F_{\ln P_s}$ are first diagnosed from the full model based on Eqs. (A5), (A6), and (A7), respectively. When running the zonally symmetric model, we transfer $F_u$, $F_T$, and $F_{\ln P_s}$ into spectral fields and then add the spectral eddy forcings to the vorticity, divergence, temperature, and logarithm surface pressure tendency terms every time step. The resulting evolution of zonal winds will be very similar to the full model.

## REFERENCES


Andrews, D. G., J. R. Holton, and C. B. Leovy, 1987: *Middle Atmosphere Dynamics*. Academic Press, 489 pp.

Birner, T., and H. Bönisch, 2010: Residual circulation trajectories and transit times into the extratropical lowermost stratosphere. *Atmos. Chem. Phys. Discuss.,* **10,** 16 837–16 860.

Boehm, M. T., and S. Lee, 2003: The implications of tropical Rossby waves for tropical tropopause cirrus formation and for the equatorial upwelling of the Brewer–Dobson circulation. *J. Atmos. Sci.,* **60,** 247–261.

Brewer, A. M., 1949: Evidence for a world circulation provided by the measurements of helium and water vapor distribution in the stratosphere. *Quart. J. Roy. Meteor. Soc.,* **75,** 351–363.

Butchart, N., and Coauthors, 2006: Simulations of anthropogenic change in the strength of the Brewer–Dobson circulation. *Climate Dyn.,* **27,** 727–741.

——, and Coauthors, 2010: Chemistry–climate model simulations of 21st century stratospheric climate and circulation changes. *J. Climate,* **23,** 5349–5374.

Chae, J. H., and S. C. Sherwood, 2007: Annual temperature cycle of the tropical tropopause: A simple model study. *J. Geophys. Res.,* **112,** D19111, doi:10.1029/2006JD007956.

Charney, J. G., and P. G. Drazin, 1961: Propagation of planetary-scale disturbances from the lower into the upper atmosphere. *J. Geophys. Res.,* **66,** 83–109.

Chen, G., R. A. Plumb, and J. Lu, 2010: Sensitivities of zonal mean atmospheric circulation to SST warming in an aqua-planet model. *Geophys. Res. Lett.,* **37,** L12701, doi:10.1029/2010GL043473.

Chen, P., and W. A. Robinson, 1992: Propagation of planetary waves between the troposphere and stratosphere. *J. Atmos. Sci.,* **49,** 2533–2545.

Deckert, R., and M. Dameris, 2008: Higher tropical SSTs strengthen the tropical upwelling via deep convection. *Geophys. Res. Lett.,* **35,** L10813, doi:10.1029/2008GL033719.

Dhomse, S., M. Weber, and J. Burrows, 2008: The relationship between tropospheric wave forcing and tropical lower stratospheric water vapor. *Atmos. Chem. Phys.,* **8,** 471–480.

Dobson, G. M. B., 1956: Origin and distribution of polyatomic molecules in the atmosphere. *Proc. Roy. Soc. London,* **236A,** 187–193.

Dunkerton, T., 1989: Nonlinear Hadley circulation driven by asymmetric differential heating. *J. Atmos. Sci.,* **46,** 956–974.

Edmon, H. J., B. J. Hoskins, and M. E. McIntyre, 1980: Eliassen–Palm cross sections for the troposphere. *J. Atmos. Sci.,* **37,** 2600–2616.

Engel, A., and Coauthors, 2008: Age of stratospheric air unchanged within uncertainties over the past 30 years. *Nat. Geosci.,* **2,** 28–31.

Fu, Q., S. Solomon, and P. Lin, 2010: On the seasonal dependence of tropical lower-stratospheric temperature trends. *Atmos. Chem. Phys.,* **10,** 2643–2653.

Garcia, R. R., and W. J. Randel, 2008: Acceleration of the Brewer–Dobson circulation due to increases in greenhouse gases. *J. Atmos. Sci.,* **65,** 2731–2739.

——, ——, and D. E. Kinnison, 2010: On the determination of age of air trends from atmospheric trace species. *J. Atmos. Sci.,* **68,** 139–154.

Garny, H., M. Dameris, and A. Stenke, 2009: Impact of prescribed SSTs on climatologies and long-term trends in CCM simulations. *Atmos. Chem. Phys.,* **9,** 6017–6031.

Geller, M. A., T. Zhou, and K. Hamilton, 2008: Morphology of tropical upwelling in the lower stratosphere. *J. Atmos. Sci.,* **65,** 2360–2374.

Gerber, E. P., and L. M. Polvani, 2009: Stratosphere–troposphere coupling in a relatively simple AGCM: The importance of stratospheric variability. *J. Climate,* **22,** 1920–1933.

Gordon, C., and W. Stern, 1982: A description of the GFDL global spectral model. *Mon. Wea. Rev.,* **110,** 625–644.

Haynes, P., C. J. Marks, M. E. McIntyre, T. G. Shepherd, and K. P. Shine, 1991: On the "downward control" of extratropical diabatic circulations by eddy-induced mean zonal forces. *J. Atmos. Sci.,* **48,** 651–678.

Holton, J. R., and C. Mass, 1976: Stratospheric vacillation cycles. *J. Atmos. Sci.,* **33,** 2218–2225.

——, P. Haynes, M. E. McIntyre, A. R. Douglass, R. B. Rood, and L. Pfister, 1995: Stratosphere–troposphere exchange. *Rev. Geophys.,* **33,** 403–439.

Kerr-Munslow, A. M., and W. A. Norton, 2006: Tropical wave driving of the annual cycle in tropical tropopause temperatures. Part I: ECMWF Analyses. *J. Atmos. Sci.,* **63,** 1410–1419.

Kirk-Davidoff, D. B., and R. S. Lindzen, 2000: An energy balance model based on potential vorticity homogenization. *J. Climate,* **13,** 431–448.

Li, F., J. Austin, and R. J. Wilson, 2008: The strength of the Brewer–Dobson circulation in a changing climate: Coupled chemistry–climate model simulations. *J. Climate,* **21,** 40–57.

Lin, P., Q. Fu, S. Solomon, and J. M. Wallace, 2009: Temperature trend patterns in Southern Hemisphere high latitudes: Novel indicators of stratospheric change. *J. Climate,* **22,** 6325–6341.

McLandress, C., and T. G. Shepherd, 2009: Simulated anthropogenic changes in the Brewer–Dobson circulation, including its extension to high latitudes. *J. Climate,* **22,** 1516–1540.

Mote, P. W., and Coauthors, 1996: An atmospheric tape recorder: The imprint of tropical tropopause temperatures on stratospheric water vapor. *J. Geophys. Res.,* **101** (95), 3989–4006.

Niwano, M., 2003: Seasonal and QBO variations of ascent rate in the tropical lower stratosphere as inferred from UARS HALOE trace gas data. *J. Geophys. Res.,* **108,** 4794, doi:10.1029/2003JD003871.

Norton, W. A., 2006: Tropical wave driving of the annual cycle in tropical tropopause temperatures. Part II: Model results. *J. Atmos. Sci.,* **63,** 1420–1431.

Plumb, R. A., 1989: On the seasonal cycle of stratospheric planetary waves. *Pure Appl. Geophys.,* **130,** 233–242.

——, 2002: Stratospheric transport. *J. Meteor. Soc. Japan,* **80,** 793–809.

——, 2010: Planetary waves and the extratropical winter stratosphere. *Dynamics, Transport and Chemistry: A Festschrift to Celebrate Alan Plumb's 60th Birthday,* L. Polvani and A. Sobel, Eds., Amer. Geophys. Union, 23–42.

——, and J. Eluszkiewicz, 1999: The Brewer–Dobson circulation: Dynamics of the tropical upwelling. *J. Atmos. Sci.,* **56,** 868–890.

Polvani, L. M., and P. J. Kushner, 2002: Tropospheric response to stratospheric perturbations in a relatively simple general circulation model. *Geophys. Res. Lett.,* **29,** 1114, doi:10.1029/2001GL014284.

Randel, W. J., 1988: The seasonal evolution of planetary waves in the Southern Hemisphere stratosphere and troposphere. *Quart. J. Roy. Meteor. Soc.,* **114,** 1385–1409.

——, R. R. Garcia, and F. Wu, 2002a: Time-dependent upwelling in the tropical lower stratosphere estimated from the zonal-mean momentum budget. *J. Atmos. Sci.,* **59,** 2141–2152.

——, F. Wu, and R. S. Stolarski, 2002b: Changes in column ozone correlated with the stratospheric EP flux. *J. Meteor. Soc. Japan,* **80,** 849–862.

——, M. Park, F. Wu, and N. Livesey, 2007: A large annual cycle in ozone above the tropical tropopause linked to the Brewer–Dobson circulation. *J. Atmos. Sci.,* **64,** 4479–4488.

——, R. R. Garcia, and F. Wu, 2008: Dynamical balances and tropical stratospheric upwelling. *J. Atmos. Sci.,* **65,** 3584–3595.

Ray, E. A., and Coauthors, 2010: Evidence for changes in stratospheric transport and mixing over the past three decades based on multiple data sets and tropical leaky pipe analysis. *J. Geophys. Res.,* **115,** D21304, doi:10.1029/2010JD014206.

Reed, R., and C. Vicek, 1969: The annual temperature variation in the lower tropical stratosphere. *J. Atmos. Sci.,* **26,** 163–167.

Rosenlof, K. H., 1995: Seasonal cycle of the residual mean meridional circulation in the stratosphere. *J. Geophys. Res.,* **100** (D3), 5173–5191.

——, and G. C. Reid, 2008: Trends in the temperature and water vapor content of the tropical lower stratosphere: Sea surface connection. *J. Geophys. Res.,* **113,** D06107, doi:10.1029/2007JD009109.

Salby, M., and P. Callaghan, 2002: Interannual changes of the stratospheric circulation: Relationship to ozone and tropospheric structure. *J. Climate,* **15,** 3673–3685.

Schoeberl, M. R., and Coauthors, 2008: QBO and annual cycle variations in tropical lower stratosphere trace gases from HALOE and Aura MLS observations. *J. Geophys. Res.,* **113,** D05301, doi:10.1029/2007JD008678.

Scinocca, J. F., and P. Haynes, 1998: Dynamical forcing of stratospheric planetary waves by tropospheric baroclinic eddies. *J. Atmos. Sci.,* **55,** 2361–2392.

Scott, R. K., 2002: Wave-driven mean tropical upwelling in the lower stratosphere. *J. Atmos. Sci.,* **59,** 2745–2759.

——, and P. Haynes, 2002: The seasonal cycle of planetary waves in the winter stratosphere. *J. Atmos. Sci.,* **59,** 803–822.

Semeniuk, K., and T. G. Shepherd, 2001a: Mechanisms for tropical upwelling in the stratosphere. *J. Atmos. Sci.,* **58,** 3097–3115.

——, and ——, 2001b: The middle-atmosphere Hadley circulation and equatorial inertial adjustment. *J. Atmos. Sci.,* **58,** 3077–3096.

Song, Y., and W. A. Robinson, 2004: Dynamical mechanisms for stratospheric influences on the troposphere. *J. Atmos. Sci.,* **61,** 1711–1725.

Sun, L., and W. A. Robinson, 2009: Downward influence of stratospheric final warming events in an idealized model. *Geophys. Res. Lett.,* **36,** L03819, doi:10.1029/2008GL036624.

——, ——, and G. Chen, 2011: The role of planetary waves in the downward influence of stratospheric final warming events. *J. Atmos. Sci.,* **68,** 2826–2843.

Taguchi, M., 2009: Wave driving in the tropical lower stratosphere as simulated by WACCM. Part I: Annual cycle. *J. Atmos. Sci.,* **66,** 2029–2043.

——, T. Yamaga, and S. Yoden, 2001: Internal variability of the troposphere–stratosphere coupled system simulated in a simple global circulation model. *J. Atmos. Sci.,* **58,** 3184–3203.

Thuburn, J., and G. C. Craig, 2000: Stratospheric influence on tropopause height: The radiative constraint. *J. Atmos. Sci.,* **57,** 17–28.

Tung, K. K., and J. S. Kinnersley, 2001: Mechanisms by which extratropical wave forcing in the winter stratosphere induces upwelling in the summer hemisphere. *J. Geophys. Res.,* **106,** 781–791.

Ueyama, R., and J. M. Wallace, 2010: To what extent does high-latitude wave forcing drive tropical upwelling in the Brewer–Dobson circulation? *J. Atmos. Sci.,* **67,** 1232–1246.

Wang, H., and M. Ting, 1999: Seasonal cycle of the climatological stationary waves in the NCEP–NCAR reanalysis. *J. Atmos. Sci.,* **56,** 3892–3919.

Yoden, S., M. Taguchi, and Y. Naito, 2002: Numerical studies on time variations of the troposphere–stratosphere coupled system. *J. Meteor. Soc. Japan,* **80,** 811–830.

Yulaeva, E., J. Holton, and J. M. Wallace, 1994: On the cause of the annual cycle in tropical lower-stratospheric temperatures. *J. Atmos. Sci.,* **51,** 169–174.

Zhou, T., M. A. Geller, and K. Hamilton, 2006: The roles of the Hadley circulation and downward control in tropical upwelling. *J. Atmos. Sci.,* **63,** 2740–2757.